Macromolecules
ARTICLE

Macromolecules **2010**, *43*, 6337–6342 **6337**
DOI: 10.1021/ma100512x

Quantum-Chemical Study of the Effect of Triethylaluminum on the Chain-End Structure, Reactivity, and Microtacticity of Poly(*N*,*N*-dimethylacrylamide) with Lithium Counterion in Nonpolar Solvents

Alexander V. Yakimansky[†] **and Axel H. E. Müller***

Makromolekulare Chemie II and Bayreuther Institut für Makromolekülforschung, Universität Bayreuth, D-95440 Bayreuth, Germany. [†]*Permanent address: Institute of Macromolecular Compounds of the Russian Academy of Sciences, Bolshoi prospect 31, 199004 St. Petersburg, Russia*

Received March 6, 2010; Revised Manuscript Received June 30, 2010

ABSTRACT: Reactions of chain growth in the anionic polymerization of *N,N*-dimethylacrylamide (DMAAm) with lithium counterion in the presence of triethylaluminum (Et_3Al) were studied using quantum-chemical DFT methods. The active sites were simulated by chain fragments consisting of two DMAAm units, the lithium counterion being coordinated to carbonyl oxygen atoms of both ultimate and penultimate units. For all local minima and transition states zero-point vibration energies and free energies, ΔG, at 200 K were calculated. It was shown that in the absence of Et_3Al *iso*-addition of the monomer to the model chain end is the most favorable, while in the presence of two Et_3Al molecules *syndio*- and *iso*-additions of DMAAm are equally probable. In the presence of one Et_3Al molecule, an unambiguous prediction of the prevailing stereomode of DMAAm addition is impossible because different stereomodes are preferred at the BHLYP/SVP (*syndio*-addition via 1LA-DAS mechanism) and BHLYP/aug-cc-pVTZ//BHLYP/SVP (*iso*-addition via 1LA-AM mechanism) levels. Thus, on the basis of the performed DFT calculations, it is possible to predict the possibility to influence the microtacticity of poly(*N,N*-dimethylacrylamide), varying the [Al]/[Li] ratio: the polymer should be predominantly isotactic at [Al]/[Li] = 0 and atactic at [Al]/[Li] ≥ 2.

Introduction

Poly(*N,N*-dimethylacrylamide) (PDMAAm) and its copolymers are prospective materials for a number of important applications. They are used in capillary electrophoresis as coatings of the capillary, improving the separations of mixtures of acidic and basic peptides[1] and DNA,[2,3] in tissue engineering for creation of designed shape cell sheets,[4] as the components of temperature-responsive materials for slow drug release,[5] as amphiphilic oligomers solubilizing fullerene into water,[6] as water-soluble viscosifiers and displacement fluids for oil recovery,[7] etc.

For all these applications, it is very important to control structural and molecular weight characteristics of PDMAAm, and the most reliable approach in this respect is anionic polymerization of *N,N*-dimethylacrylamide (DMAAm). It is known that the anionic polymerization of DMAAm by organolithium initiators in both hydrocarbons[8] and THF[9−11] is not well controlled, even in the presence of σ-donor additives, such as TMEDA,[11] due to formation of insoluble, highly crystalline polymers with highly isotactic microstructure.[8−10,12,13,14a]

Recently, to control the polymerization of DMAAm, new effective anionic initiating systems were developed, consisting of organometallic compounds of alkali and alkaline earth metals modified by electron acceptor Lewis acids (LA), such as Et_3B,[10a,14b] Et_2Zn,[10,12,13,14b] and Et_3Al.[14] It has been found that in the presence of Lewis acids soluble and highly syndiotactic[10] or heterotactic[10,14a] polymers are formed with predictable molecular weight and narrow molecular weight distribution[10,12,13] even at 30 °C.[10a]

*Corresponding author. E-mail: axel.mueller@uni-bayreuth.de.

The anionic polymerization of *N,N*-diethylacrylamide (DEAAm) is controlled by Lewis acids in a similar way.[10b] The corresponding polymers show lower critical solution temperature (LCST) behavior in water close to body temperature, which makes them very attractive materials for biological and medical applications.[15a,b] Anionic polymerization of DEAAm was performed from a poly(*tert*-butyl acrylate)−Li macroinitiator in the presence of a 7-fold excess of Et_3Al.[15c] Thermo- and pH-responsive micelles of poly(acrylic acid)-*block*-PDEAAm were prepared after the hydrolysis of the poly(*tert*-butyl acrylate) block.

Recent kinetic data on the polymerization of DEAAm in THF in the presence of Et_3Al showed that the chain-growth reaction probably involves activation of the monomer molecule by coordination to the Lewis acid.[16] DFT calculations performed in relation to this data[17] have demonstrated that in these systems external solvation of lithium counterions with THF molecules is more favorable than the intramolecular lithium complexation to carbonyl oxygen atoms of the penultimate or/and antepenultimate unit.

In nonpolar solvents, such as toluene, such intramolecular complexation should predominate, affecting both the reactivity of active chain ends and, possibly, the microtacticity of the obtained polymers. For the anionic polymerization of DMAAm by dibutylmagnesium, it was found that the isotactic triad content is almost the same in THF and toluene.[9] This contradicts earlier data that a lower dielectric constant of the medium leads to higher isotacticity of PDMAAm synthesized by anionic polymerization from organometallic compounds of both alkali and alkaline earth metals.[8] However, up to now there are no experimental data on polymerization of *N,N*-dialkylacrylamides in nonpolar media with lithium counterion in the presence of Et_3Al.

Published on Web 07/15/2010

This paper attempts to obtain a theoretical insight into the problem and presents some predictions made on the basis of quantum-chemical DFT calculations.

Methods of Computation

All calculations were performed using the TURBOMOLE program.[18] Density functional theory (DFT) was employed. It is much more suitable and economic approach for very large and computer time-consuming systems studied here than *ab initio* methods because DFT takes into account electron correlation effects directly. The numerical integration scheme using a "m3"-grid has been described in ref 19. The geometry optimizations have been carried out using a *split valence* (SV) basis set augmented with polarization functions for non-hydrogen atoms. This basis (which is comparable to a 6-31G*) is referred to as SVP.[20]

The BHLYP hybrid potential, combining BH exchange potential with 50% of nonlocal Hartree−Fock exchange explicitly taken into account[21] and the LYP correlation potential,[22] has been used. The choice of this potential was based on the following considerations. The chain-growth reactions studied here represent 1,4-additions of lithium enolates (in our case, PDMAAm-active chain ends) to conjugated carbonyl compounds (in our case, *N,N*-dimethylacrylamide monomer molecule). Therefore, we tried to use different exchange-correlation potentials, including BP86,[23,24] B3LYP,[22,25] and BHLYP, to reproduce correctly the geometries of eight-membered cyclic transition states of 1,4-addition of acetaldehyde lithium enolate to acrolein.[26] However, both BP86 and B3LYP failed to find a saddle point in the vicinity of the initial geometry guess for the addition of acetaldehyde lithium enolate to acrolein. This failure is, obviously, due to the lack of nonlocal Hartree−Fock exchange in both BP86 (no Hartree−Fock exchange) and B3LYP (25% of Hartree−Fock exchange). In contrast, with BHLYP potential (50% of Hartree−Fock exchange), the transition state of the addition of acetaldehyde lithium enolate to acrolein was successfully localized.

For all structures calculated at the BHLYP/SVP level, zero point vibration energies and entropies were calculated at temperature 200 K, at which anionic polymerization of *N,N*-dialkylacrylamides is most frequently performed. All local minimum structures have no imaginary vibration frequencies, and all transition states have exactly one imaginary vibration frequency. Initial geometries for the eight-membered cyclic cores of the calculated transition states were taken from ref 26, in which the reaction between acetaldehyde lithium enolate and acrolein was studied at the *ab initio* 3-21G level.

For all calculated structures, single point energy calculations were performed at the BHLYP/aug-cc-pVTZ//BHLYP/SVP level, using the TURBOMOLE diffuse function augmented correlation consistent triple-zeta plus polarization basis set (aug-cc-pVTZ).[27]

Results and Discussion

The reaction between the dimeric chain-end model and the DMAAm molecule in the absence of a Lewis acid, leading to the formation of the trimeric chain end, was studied, as shown in Scheme 1. Chiral carbon atoms are marked with a star. The second chiral carbon atom, being formed in the product, the trimeric chain end, may have the same or the opposite configuration with respect to the first chiral carbon atom in the initial dimeric chain-end model, giving rise to an *iso*- or *syndio*-triad, respectively. In these chain-end models, the lithium ion is intramolecularly coordinated to the carbonyl oxygen atoms of penultimate (in the dimeric and trimeric models) and antepenultimate (in the trimeric model) units which should be the major motif, forming the lithium surrounding in nonpolar media in the absence of external electron donor ligands.

Scheme 1. Reaction between the Dimeric Chain-End Model and DMAAm

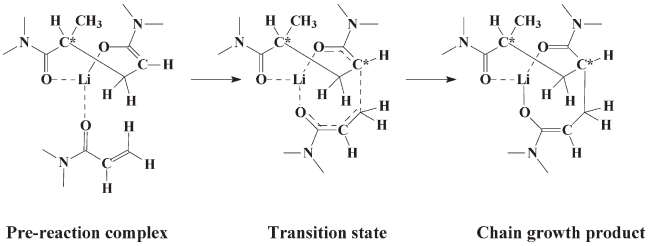

Scheme 2. "Deactivated Active Site" (DAS) Mechanism

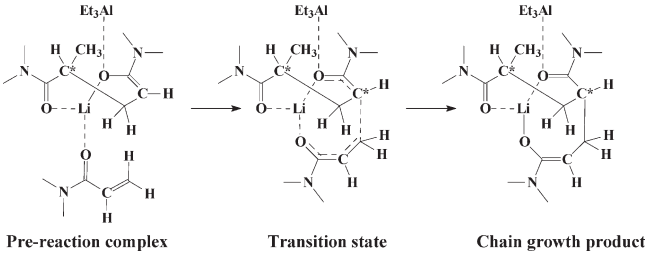

Scheme 3. "Activated Monomer" (AM) Mechanism

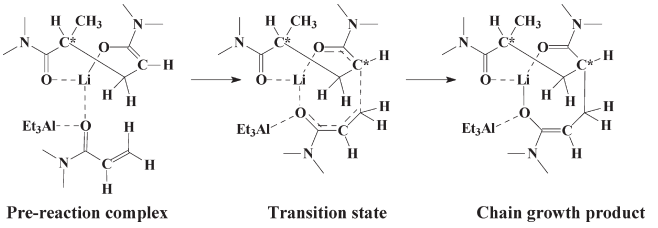

Scheme 4. Reaction between the Dimeric Chain-End Model and DMAAm Molecule in the Presence of Two Triethylaluminum Molecules

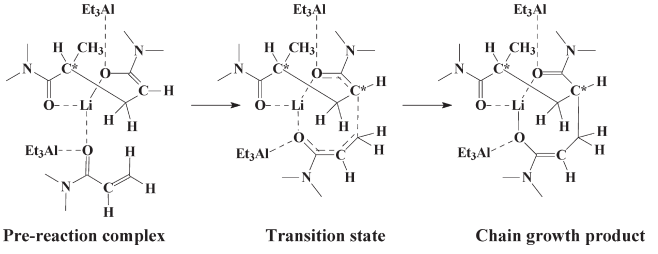

We studied the model chain growth reaction in the presence of one Et_3Al molecule, coordinated either to the active site of the initial dimeric chain-end model ("deactivated active site" (DAS) mechanism, Scheme 2) or to the incoming monomer molecule ("activated monomer" (AM) mechanism, Scheme 3) as well as in the presence of two Et_3Al molecules coordinated to both the active site and incoming monomer (Scheme 4). Below, the sets of data for the reactions presented in Schemes 1−4 are marked as 0LA, 1LA-DAS, 1LA-AM, and 2LA, respectively.

The geometries of all prereaction complexes and chain growth products were obtained from the geometries of the corresponding transition states by shifting from a transition state geometry "backward" and "forward" along the transition vector direction and a subsequent complete reoptimization of the shifted geometries. The transition vector structure corresponded in all cases to the formation of a new C−C bond between the active site and monomer molecules. The value of the newly forming C−C bond

Table 1. Calculated Values of Absolute Total Energies, E, Relative Total Energies, ΔE, Sum of the Entropic Contribution (at 200 K) and Zero Point Vibration Energy, $G - E$, and Relative Free Energies, ΔG, at the BHLYP/SVP and BHLYP/aug-cc-pVTZ//BHLYP/SVP (Bold) Levels for the 0LA Mechanism of the Reaction between the Dimeric Chain-End Model and DMAAm Molecule

	iso-addition					*syndio*-addition				
structure (Scheme *1*)	E, hartree	$E + E[(Et_3Al)_2]$, hartree[a]	ΔE, kcal/mol	$G - E$, kcal/mol	ΔG, kcal/mol	E, hartree	$E + E[(Et_3Al)_2]$, hartree[a]	ΔE, kcal/mol	$G - E$, kcal/mol	ΔG, kcal/mol
$(Et_3Al)_2$	−959.323 962			208.16		−959.323 962			208.16	
	−960.092 391					**−960.092 391**				
prereaction complex	−984.611 916	−1943.935 878	28.72	434.98	14.89	−984.604 205	−1943.928 167	33.56	435.46	20.21
	−985.753 161	**−1945.845 551**	**19.22**			**−985.745 595**	**−1945.837 986**	**23.96**		
transition state	−984.595 392	−1943.919 354	39.10	437.22	27.51	−984.590 428	−1943.914 390	42.21	437.55	30.95
	−985.734 481	**−1945.826 872**	**30.94**			**−985.729 087**	**−1945.821 478**	**34.32**		
chain growth product	−984.619 204	−1943.943 166	24.15	438.16	13.50	−984.614 402	−1943.938 364	27.16	439.70	18.05
	−985.756 412	**−1945.848 802**	**17.18**			**−985.751 227**	**−1945.843 617**	**20.43**		

[a] To the values of E and $G - E$, the corresponding values for the $(Et_3Al)_2$ dimer is added (1) to make the absolute total and free energy values comparable to those presented in Table 4 and (2) to take into account the fact that triethylaluminum is dimerized in nonpolar solvents.[28]

Table 2. Calculated Values of Absolute Total Energies, E, Relative Total Energies, ΔE, Sum of the Entropic Contribution (at 200 K) and Zero Point Vibration Energy, $G - E$, and Relative Free Energies, ΔG, at the BHLYP/SVP and BHLYP/aug-cc-pVTZ//BHLYP/SVP (Bold) Levels for the 1LA-DAS Mechanism of the Reaction between the Dimeric Chain-End Model and DMAAm Molecule

	iso-addition					*syndio*-addition				
structure (Scheme *2*)	E, hartree	$E + {}^1/_2E[(Et_3Al)_2]$, hartree*	ΔE, kcal/mol	$G - E$, kcal/mol	ΔG, kcal/mol	E, hartree	$E + {}^1/_2E[(Et_3Al)_2]$, hartree*	ΔE, kcal/mol	$G - E$, kcal/mol	ΔG, kcal/mol
prereaction complex	−1464.320 211	−1943.982 192	−0.34	439.64	−9.51	−1464.324 035	−1943.986 016	−2.74	439.45	−12.10
	−1465.838 877	**−1945.885 072**	**−5.59**			**−1465.843 440**	**−1945.889 635**	**−8.45**		
transition state (Figure *3*)	−1464.289 099	−1943.951 08	19.18	442.52	12.89	−1464.292 921	−1943.954 902	16.79	442.67	10.65
	−1465.803 620	**−1945.849 815**	**16.54**			**−1465.807 935**	**−1945.854 131**	**13.83**		
chain growth product	−1464.308 507	−1943.970 488	7.00	444.14	2.33	−1464.311 503	−1943.973 484	5.12	444.67	0.98
	−1465.821 996	**−1945.868 191**	**5.01**			**−1465.825 236**	**−1945.871 432**	**2.97**		

* To the values of E and $G - E$, half of the corresponding values for the $(Et_3Al)_2$ dimer is added (1) to make the absolute total and free energy values comparable to those presented in Table 4 and (2) to take into account the fact that triethylaluminum is dimerized in nonpolar solvents.[28]

is ∼4, 2.0−2.5, and ∼1.55 Å in prereaction complexes (PRC), transition states (TS), and chain growth products, respectively. Therefore, the transformations from the considered prereaction complexes to the corresponding chain-growth products are one-step reactions. The found transition states connect the correct reactant and product geometries.

It is clear from Scheme 2 for the DAS mechanism that the Lewis acid molecule, being initially located at the active site of the reagent dimeric chain-end model, is coordinated to the carbonyl oxygen atom of the penultimate unit in the product trimeric chain-end model. Similarly, Scheme 3 for the AM mechanism shows that the Lewis acid molecule is located at the incoming monomer molecule which further transforms into the active site of the product trimeric chain-end model.

It should be noted that the ratio of rate constants of *iso*- and *syndio*-additions for each of the considered mechanisms is determined not only by the difference $\Delta G^{\ddagger}(iso) - \Delta G^{\ddagger}(syndio)$ in the corresponding activation free energies, $\Delta G^{\ddagger}(iso) = \Delta G(iso\text{-TS}) - \Delta G(iso\text{-PRC})$ and $\Delta G^{\ddagger}(syndio) = \Delta G(syndio\text{-TS}) - \Delta G(syndio\text{-PRC})$, but also by the relative populations of the corresponding prereaction complexes, *iso*-PRC and *syndio*-PRC, involved in an equilibrium through the following reversible reactions

$$iso\text{-PRC} \rightleftarrows \text{DMAAm} + \text{active site} \rightleftarrows syndio\text{-PRC}$$

and defined by the difference $\Delta G(iso\text{-PRC}) - \Delta G(syndio\text{-PRC})$. Therefore, the ratios of rate constants of *iso*- and *syndio*-additions are determined by relative positions of the corresponding transition states, i.e., by the $\Delta G(iso\text{-TS}) - \Delta G(syndio\text{-TS})$ values.

Tables 1−4 present the calculated values of absolute total energies and relative total and free energies for all structures shown in Schemes 1−4 for both *iso*- and *syndio*-additions. These results are visualized as diagrams of the ΔE and ΔG values for the 0LA, 1LA-DAS, 1LA-AM, and 2LA mechanisms of the chain growth (Figures 1 and 2).

It is seen from Figures 1 and 2 that addition of one or two Et_3Al molecules catalyzes the chain growth process for 1LA-DAS, 1LA-AM, and 2LA mechanisms, as compared to the Lewis acid-free reaction (0LA mechanism). This is due to the fact that the Lewis acid stabilizes the chain growth reaction transition states, being attached to the active site of the initial dimeric model and/or to the incoming monomer molecule.

Activation energies, $\Delta E^{\ddagger} = \Delta E(\text{TS}) - \Delta E(\text{PRC})$, and activation free energies, $\Delta G^{\ddagger} = \Delta G(\text{TS}) - \Delta G(\text{PRC})$, for the 1LA-DAS (Table 2) and 1LA-AM mechanisms (Table 3) are respectively higher and lower than that for the 0LA chain growth reaction (Table 1). This could be explained as follows. For the 1LA-DAS mechanism, the carbonyl oxygen of the initial dimeric model becomes less nucleophilic in the transition state compared to the prereaction complex. Therefore, the Lewis acid coordination to this oxygen atom is less stabilizing for the transition state than for the prereaction complex. In contrast, for the 1LA-AM mechanism, the carbonyl oxygen of the incoming monomer molecule becomes more nucleophilic in the transition state compared to the prereaction complex. As a result, the transition state of the 1LA-AM mechanism is more strongly stabilized by the coordination of Et_3Al to this oxygen atom than the prereaction complex.

For the 2LA chain growth reaction (Table 4), the $\Delta E^{\ddagger}$ and $\Delta G^{\ddagger}$ values for both *iso*- and *syndio*-additions are higher than the corresponding values for the 1LA-AM mechanism (Table 3) and lower than those for the 1LA-DAS mechanism (Table 2). It means that for the 2LA mechanism the decrease in the $\Delta E^{\ddagger}$ and

Table 3. Calculated Values of Absolute Total Energies, E, Relative Total Energies, ΔE, Sum of the Entropic Contribution (at 200 K) and Zero Point Vibration Energy, $G - E$, and Relative Free Energies, ΔG, at the BHLYP/SVP and BHLYP/aug-cc-pVTZ//BHLYP/SVP (Bold) Levels for the 1LA-AM Mechanism of the Reaction between the Dimeric Chain-End Model and DMAAm Molecule

	iso-addition					*syndio*-addition				
structure (Scheme *3*)	E, hartree	$E + {}^1/_2E[(Et_3Al)_2]$, hartree[a]	ΔE, kcal/mol	$G - E$, kcal/mol	ΔG, kcal/mol	E, hartree	$E + {}^1/_2E[(Et_3Al)_2]$, hartree[a]	ΔE, kcal/mol	$G - E$, kcal/mol	ΔG, kcal/mol
prereaction complex	−1464.294 681	−1943.956 662	15.68	438.67	5.54	−1464.290 519	−1943.952 500	18.29	440.66	10.14
	−1465.815 175	**−1945.861 370**	**9.29**			**−1465.810 343**	**−1945.856 538**	**12.32**		
transition state (Figure *4*)	−1464.289 632	−1943.951 613	18.85	441.57	11.61	−1464.281 243	−1943.943 224	24.11	442.69	17.99
	−1465.809 547	**−1945.855 743**	**12.82**			**−1465.799 563**	**−1945.845 758**	**19.09**		
chain growth product	−1464.338 609	−1944.000 59	−11.89	444.59	−16.11	−1464.334 801	−1943.996 782	−9.50	444.64	−13.67
	−1465.852 563	**−1945.898 758**	**−14.18**			**−1465.848 025**	**−1945.894 220**	**−11.33**		

[a] To the values of E and $G - E$, half of the corresponding values for the $(Et_3Al)_2$ dimer is added (1) to make the absolute total and free energy values comparable to those presented in Table 4 and (2) to take into account the fact that triethylaluminum is dimerized in nonpolar solvents.[28]

Table 4. Calculated Values of Absolute Total Energies, E, Relative Total Energies, ΔE, Sum of the Entropic Contribution (at 200 K) and Zero Point Vibration Energy, $G - E$, and Relative Free Energies, ΔG, at the BHLYP/SVP and BHLYP/aug-cc-pVTZ//BHLYP/SVP (Bold) Levels for the 2LA Mechanism of the Reaction between the Dimeric Chain-End Model and DMAAm Molecule

	iso-addition				*syndio*-addition			
structure (Scheme *4*)	E, hartree	ΔE, kcal/mol	$G - E$, kcal/mol	ΔG, kcal/mol	E, hartree	ΔE, kcal/mol	$G - E$, kcal/mol	ΔG, kcal/mol
prereaction complex	−1943.993 763	−7.60	445.34	−11.07	−1943.996 464	−9.30	446.58	−11.53
	−1945.891964	**−9.91**			**−1945.894989**	**−11.81**		
transition state (Figure *5*)	−1943.981 261	0.24	448.69	0.12	−1943.981 647	0	448.81	0
	−1945.875635	**0.34**			**−1945.876170**	**0**		
chain growth product	−1944.014 247	−20.46	448.85	−20.42	−1944.018 804	−23.32	450.76	−21.37
	−1945.906065	**−18.76**			**−1945.910642**	**−21.63**		

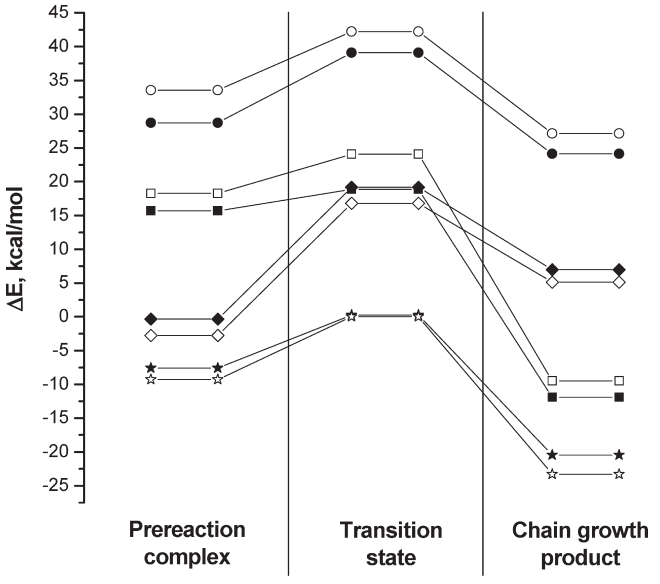

Figure 1. ΔE values of the stationary points calculated at the BHLYP/SVP level for the considered chain growth reaction via the 0LA mechanism (circles), 1LA-DAS mechanism (diamonds), 1LA-AM mechanism (squares), and 2LA mechanism (stars) for *iso*- (solid symbols) and *syndio*- (open symbols) DMAAm additions to the active site.

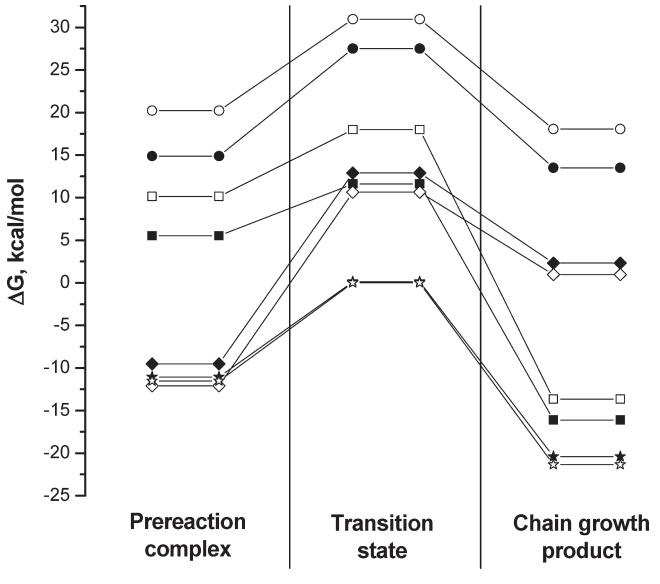

Figure 2. ΔG values of the stationary points calculated at the BHLYP/SVP level for the considered chain growth reaction via the 0LA mechanism (circles), 1LA-DAS mechanism (diamonds), 1LA-AM mechanism (squares), and 2LA mechanism (stars) for *iso*- (solid symbols) and *syndio*- (open symbols) DMAAm additions to the active site.

$\Delta G^{\ddagger}$ values due to the activation of the incoming monomer by coordination of one LA exceeds the decrease in the $\Delta E^{\ddagger}$ and $\Delta G^{\ddagger}$ values due to the deactivation of the active site by coordination of the other LA molecule.

Comparing the data for the 1LA-DAS and 1LA-AM mechanisms presented in Figures 1 and 2, one can see that the 1LA-DAS prereaction complexes are lower both in energy and in free energy than those for the 1LA-AM mechanism. This is due to the fact that in all the prereaction complexes the enolate oxygen atom of the active site is more nucleophilic than the oxygen atom of the monomer molecule.

It should be noted that the ΔE values for the 2LA prereaction complexes and chain growth products are systematically lower than those for the corresponding 1LA-DAS structures (Figure 1). The same tendency is observed for the ΔG values of the 2LA and 1LA-DAS chain growth products (Figure 2). However, ΔG values for the 2LA prereaction complexes are close to those for the 1LA-DAS ones (Figure 2). It means that the energy gain due

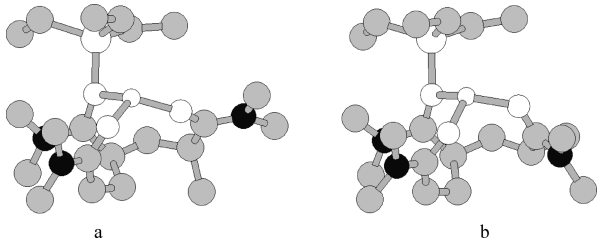

Figure 3. DFT optimized transition states for *iso*-addition (a) and *syndio*-addition (b) via the 1LA-DAS mechanism. Carbon atoms are gray circles, nitrogen atoms are black circles, lithium atoms are small white circles, oxygen atoms are intermediate white circles, and aluminum atoms are large white circles. Hydrogen atoms are not shown.

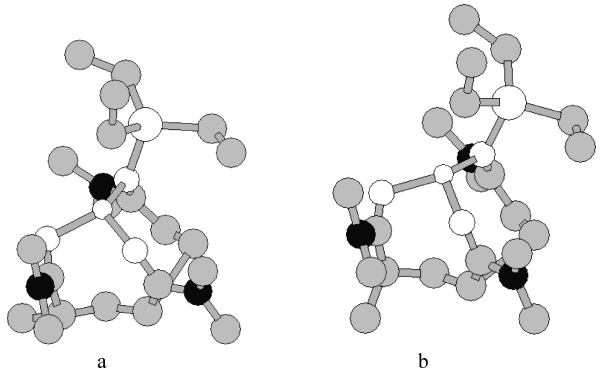

Figure 4. DFT optimized transition states for *iso*-addition (a) and *syndio*-addition (b) via the 1LA-AM mechanism. For assignments see Figure 3.

to addition of the second LA molecule to the 1LA-DAS prereaction complex is almost compensated for by unfavorable entropic contribution into free energy.

It is seen from Tables 1−4 that above-mentioned relationships between the ΔE values of all considered structures at the BHLYP/SVP level are qualitatively reproduced in the calculations with diffuse function augmented basis set at the BHLYP/aug-cc-pVTZ//BHLYP/SVP level.

The ratios of the rate constants for the chain growth reactions via the 0LA, 1LA-DAS, 1LA-AM, and 2LA mechanisms are determined by the relative positions of the corresponding transition state levels. It is helpful to determine the most preferable mechanism and the stereomode (*iso*- or *syndio*-) of the chain growth at different amounts of the added LA, i.e., at different [Al]/[Li] ratios.

If no LA is added (0LA chain growth reaction), then the most favorable is *iso*-addition of DMAAm molecule to the dimeric chain-end model because the ΔE and ΔG values for its transition state structure are lower by ca. 3.0 and 3.5 kcal/mol, respectively, than the corresponding values for *syndio*-addition (Table 1). This result is predicted at both BHLYP/aug-cc-pVTZ//BHLYP/SVP and BHLYP/SVP levels.

At [Al]/[Li] = 1, the most preferable modes of the chain growth are different for the 1LA-DAS and 1LA-AM mechanisms. For the 1LA-DAS mechanism (Table 2), the transition state for *syndio*-addition (Figure 3b) has lower ΔE and ΔG values than those for the *iso*-addition transition state (Figure 3a). In contrast, for the 1LA-AM mechanism (Table 3), the transition state for *iso*-addition (Figure 4a) is more favorable than the transition state structure corresponding to the *syndio*-addition (Figure 4b). It should be noted that this result is qualitatively the same at both at both BHLYP/SVP and BHLYP/aug-cc-pVTZ//BHLYP/SVP levels.

At the BHLYP/SVP level, the ΔE and ΔG values for the transition state of *syndio*-addition via the 1LA-DAS mechanism

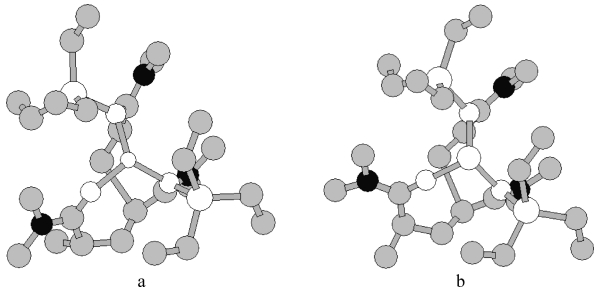

Figure 5. DFT optimized transition states for *iso*-addition (a) and *syndio*-addition (b) via the 2LA mechanism. For assignments see Figure 3.

(16.8 and 10.7 kcal/mol, respectively, Table 2) are lower than those for the transition state of *iso*-addition via 1LA-AM mechanism (18.9 and 11.6 kcal/mol, respectively, Table 3). However, at the BHLYP/aug-cc-pVTZ//BHLYP/SVP level, the opposite result is obtained: the ΔE value for the transition state of *syndio*-addition via the 1LA-DAS mechanism (13.8 kcal/mol, Table 2) is slightly higher than that for the transition state of *iso*-addition via 1LA-AM mechanism (12.8 kcal/mol, Table 3). Therefore, a definite conclusion of the preferred stereomode of addition is not possible at [Al]/[Li] = 1.

At [Al]/[Li] = 2 (2LA chain growth reaction), as seen from Figures 1, 2, and Table 4, the transition states for *iso*- and *syndio*-additions (Figure 5, a and b, respectively) have almost equal energies, the differences being ca. 0.2−0.3 kcal/mol for ΔE and 0.1 kcal/mol for ΔG, which is less than kT at 200 K. Calculations at the BHLYP/SVP and BHLYP/aug-cc-pVTZ//BHLYP/SVP levels give virtually the same results. Therefore, in this case *syndio*- and *iso*-additions of DMAAm to the active site have close probabilities.

Conclusions

DFT calculations of stationary points (prereaction complexes, transition states, and reaction products) have been calculated for the reactions of *iso*- and *syndio*-additions of DMAAm to the dimeric chain-end model of PDMAAm with lithium counterion. The influence of Et_3Al molecule(s) complexed to the oxygen atom of the active site ("deactivated active site" mechanism) or/and to the carbonyl oxygen of DMAAm ("activated monomer" mechanism) on the activation energy of the chain-growth reaction, and the most preferable stereomode of DMAAm addition was studied. We conclude that in the absence of Et_3Al (0LA mechanism) *iso*-addition of the monomer to the model chain end is more favorable than *syndio*-addition, while in the presence of two LA molecules (2LA mechanism) *syndio*- and *iso*-additions of DMAAm are equally probable. In the presence of one Et_3Al molecule, an unambiguous prediction of the prevailing stereomode of DMAAm addition is hardly possible because different stereomodes are preferred at the BHLYP/SVP (*syndio*-addition via 1LA-DAS mechanism) and BHLYP/aug-cc-pVTZ//BHLYP/SVP (*iso*-addition via 1LA-AM mechanism) levels.

These results imply that the anionic polymerization of DMAAm in a nonpolar solvent in the absence of LA additives ([Al]/[Li] = 0) should lead to a predominantly isotactic PDMAAm, while the resulting PDMAAm should be mainly atactic at [Al]/[Li] ≥ 2.

Acknowledgment. A.V.Y. is grateful to Deutsche Forschungsgemeinschaft for financial support.

Supporting Information Available: Optimized Cartesian coordinates as input files for visualization with the HYPERCHEM software (extension .hin) for all calculated structures. This

material is available free of charge via the Internet at http://pubs.acs.org.

References and Notes

(1) Wang, Y.; Hu, S.; Li, H.; Allbritton, N. L.; Sims, C. E. *J. Chromatogr. A* **2003**, *1004*, 61.
(2) Albarghouthi, M. N.; Buchholz, B. A.; Doherty, E. A. S.; Bogdan, F. M.; Zhou, H.; Barron, A. E. *Electrophoresis* **2001**, *22*, 737.
(3) Ren, J.; Ulvik, A.; Refsum, H.; Ueland, P. M. *Anal. Biochem.* **1999**, *276*, 188.
(4) Hirose, M.; Kwon, O. H.; Yamato, M.; Kikuchi, A.; Okano, T. *Biomacromolecules* **2000**, *1*, 377.
(5) Aoki, T.; Kawashima, M.; Katono, H.; Sanui, K.; Igata, N.; Okano, T.; Sakurai, Y. *Macromolecules* **1994**, *27*, 947.
(6) Sawada, H.; Iidzuka, J.; Maekawa, T.; Takahashi, R.; Kawase, T.; Oharu, K.; Nakagawa, H.; Ohira, K. *J. Colloid Interface Sci.* **2003**, *263*, 1.
(7) (a) McCormick, C. L.; Elliot, D. L. *Macromolecules* **1986**, *19*, 542. (b) McCormick, C. L.; Chen, G. S. *J. Polym. Sci., Part A* **1984**, *22*, 3633.
(8) Butler, K.; Thomas, P. R.; Tyler, G. J. *J. Polym. Sci.* **1960**, *48*, 357.
(9) Nakhmanovich, B. I.; Urman, Ya. G.; Arest-Yakubovich, A. A. *Macromol. Chem. Phys.* **2001**, *202*, 1327.
(10) (a) Kobayashi, M.; Ishizone, T.; Nakahama, S. *Macromolecules* **2000**, *33*, 4411. (b) Kobayashi, M.; Okuyama, S.; Ishizone, T.; Nakahama, S. *Macromolecules* **1999**, *32*, 6466.
(11) Xie, X.; Hogen-Esch, T. E. *Macromolecules* **1996**, *29*, 1746.
(12) Nakahama, S.; Kobayashi, M.; Ishizone, T.; Hirao, A.; Kobayashi, M. *J. Macromol. Sci., Pure Appl. Chem.* **1997**, *A34*, 1845.
(13) Kobayashi, M.; Ishizone, T.; Hirao, A.; Nakahama, S.; Kobayashi, M. *Polym. Mater. Sci. Eng.* **1997**, *76*, 304.
(14) (a) Nakhmanovich, B. I.; Urman, Ya. G.; Krystal'nyi, E. V.; Arest-Yakubovich, A. A. *Polym. Sci., Ser. B* **2003**, *45*, 135. (b) Martinez-Castro, N.; Zhang, M.; Pergushov, D. V.; Müller, A. H. E. *Des. Monomers Polym.* **2006**, *9*, 63.
(15) (a) Park, T. G.; Hoffman, A. S. *J. Appl. Polym. Sci.* **1992**, *46*, 659. (b) Eggert, M.; Freitag, R. *J. Polym. Sci., Part A: Polym. Chem.* **1994**, *32*, 3019. (c) André, X.; Zhang, M.; Müller, A. H. E. *Macromol. Rapid Commun.* **2005**, *26*, 558.
(16) André, X.; Benmohamed, Kh.; Yakimansky, A. V.; Litvinenko, G. I.; Müller, A. H. E. *Macromolecules* **2006**, *39*, 2773.
(17) Yakimansky, A. V.; Müller, A. H. E. *Macromolecules* **2006**, *39*, 4228.
(18) Häser, M.; Ahlrichs, R.; Baron, H. P.; Weis, P.; Horn, H. *Theor. Chim. Acta* **1992**, *83*, 455.
(19) Treutler, O.; Ahlrichs, R. *J. Chem. Phys.* **1995**, *102*, 346.
(20) Schäfer, A.; Horn, H.; Ahlrichs, R. *J. Chem. Phys.* **1992**, *97*, 2571.
(21) Becke, A. D. *J. Chem. Phys.* **1993**, *98*, 1372.
(22) Lee, C.; Yang, W.; Parr, R. G. *Phys. Rev. B* **1988**, *37*, 785.
(23) Becke, A. D. *Phys. Rev. A* **1988**, *38*, 3098.
(24) Perdew, J. P. *Phys. Rev. B* **1986**, *33*, 8822.
(25) Becke, A. D. *J. Chem. Phys.* **1993**, *98*, 5648.
(26) Bernardi, A.; Capelli, A. M.; Cassinari, A.; Comotti, A.; Gennari, C.; Scolastico, C. *J. Org. Chem.* **1992**, *57*, 7029.
(27) Dunning, T. H.; Peterson, K. A.; Wilson, A. K. *J. Chem. Phys.* **2001**, *114*, 9244.
(28) Schmitt, B.; Schlaad, H.; Müller, A. H. E.; Mathiasch, B.; Steiger, S.; Weiss, H. *Macromolecules* **2000**, *33*, 2887.